VOLUME 122, NUMBER 47
NOVEMBER 29, 2000

JOURNAL OF THE AMERICAN CHEMICAL SOCIETY

Application of Atomic Pair Distribution Function Analysis to Materials with Intrinsic Disorder. Three-Dimensional Structure of Exfoliated-Restacked WS_2: Not Just a Random Turbostratic Assembly of Layers

Valeri Petkov,[†] Simon J. L. Billinge,*[,†] Joy Heising,[‡] and Mercouri G. Kanatzidis*[,‡]

Contribution from the Department of Physics and Astronomy and Center for Fundamental Materials Research and Department of Chemistry and Center for Fundamental Materials Research, Michigan State University, East Lansing, Michigan 48823

Received June 8, 2000

Abstract: The *three-dimensional* structure of metastable exfoliated-restacked WS_2 (r-WS_2) has been determined by the atomic pair distribution function (PDF) technique. We show that the structure of r-WS_2 is not a random turbostratic assembly of layers, as previously thought, but it can be better regarded as a monoclinic structure with considerable intrinsic disorder. At room temperature, the atomic-scale structure of r-WS_2 is well described in the space group $P112_1$ of the monoclinic system with four formula units in the cell, and lattice parameters $a = 3.270(5)$ Å, $b = 5.717(5)$ Å, $c = 12.309(5)$ Å, and $\gamma = 88.43°$. Analysis of the X-ray scattering data, collected with Synchrotron radiation ($\lambda = 0.202$ Å) over a wide scattering angle, shows that the metastable material is built of layers of distorted (WS_6) octahedral units, in contrast to hexagonal 2H-WS_2 which is built of layers of perfect (WS_6) trigonal prisms. A characteristic structural feature of the restacked material is that *W* atoms within a single layer form *zigzag* chains along the *a* axis of the unit cell via short metal−metal bonds of length 2.77(1) and 2.85(1) Å, in agreement with previous two-dimensional electron diffraction studies.

1.Introduction

Metal dichalcogenides, in particular MoS_2 and WS_2, are known to possess a unique combination of valuable properties which make them useful as solid lubricants[1] and more important as indispensable industrial catalysts for hydrodesulfurization of crude oil.[2] The chemistry of MS_2 (M = Mo, W) is fascinating since both materials can be manipulated to form a suspension of single (MS_2) layers which can be restacked, with foreign species included if desired.[3−6] In this way, so-called lamellar nanocomposites can be formed in which the inorganic metal−sulfide matrix is combined with guest molecules or polymers

[†] Department of Physics and Astronomy and Center for Fundamental Materials Research.

[‡] Department of Chemistry and Center for Fundamental Materials Research.

(1) (a) Zhou, Z. R.; Vincent, L. *WEAR* **1999**, *229* (2), 962−967. (b) Donnet, C.; Martin, J. M.; LeMogne, T.; Belin, M. *Tribol. Int.* **1996**, *29* (2), 123−128. (c) Genut, M.; Margulis, L.; Hodes, G.; Tenne, R. *Thin Solid Films* **1992**, *217* (1−2), 91−97. (d) Heshmat, H.; Brewe, D. E. *J. Tribol-T ASME* **1996**, *118* (3), 484−491. (e) Fleischauer, P. D. *Thin Solid Films* **1987**, *154*, 309.

(2) (a) Harris, S.; Chianelli, R. R. *J. Catal.* **1984**, *86*, 400. (b) Asudevan, P. T.; Fierro, J. L. G. A review of hydrodesulfurization catalysis. *Catal Rev.* **1996**, *38* (2), 161−188. (d) Zdrazil, M. The Chemistry of the Hydrodesulfurization Process (Review). *Appl. Catal.* **1982**, *4* (2), 107−125.

(3) Yang, D.; Sandoval, S. J.; Divigalpitiya, W. M. R.; Irwin, J. C.; Frindt, R. F. *Phys. Rev.* **1991**, *B14*, 12053.

(4) Yang, D.; Frindt, R. F. *J. Phys. Chem. Solids* **1996**, *57*, 1113.

(5) Tsai, H.-L.; Heising, J.; Schindler, J. L.; Kannewurf, C. R.; Kanatzidis, M. G. *Chem. Mater.* **1997**, *9*, 879.

(6) Divigalpitiya, W. M. R.; Frindt, R. F.; Morrison, S. R. *Science* **1989**, *246*, 369.

10.1021/ja002048i CCC: $19.00
Published on Web 11/10/2000

on a nanometer scale.[7] Of course, this property of MoS_2 and WS_2 is strongly associated with their layered structure. The materials are hexagonal and may be considered as built of layers of edge-sharing perfect (MS_6) trigonal prisms stacked along the *c*-axis of the unit cell.[8,9] The strong covalent bonding between metal and sulfur atoms in the layers and the relatively weak van der Waals interaction between the layers are what gives these materials their useful properties and renders them good hosts suitable for intercalation/encapsulation chemistry. For example, species with Li ions intercalated between the layers are formed when MS_2 is treated with *n*-butyllithium. After undergoing a redox reaction with water, the materials can be exfoliated with the (MS_2) monolayers remaining separate from one another and suspended in solution for days. The monolayers can be "restacked" by filtration, precipitation, centrifugation, or evaporation to form bulk material.[4,5] The chemical composition of the material obtained and the relationship between charge on the single (WS_2) layers and structure of bulk r-WS_2 have been discussed extensively recently.[10] It was found that the actual sample composition is Li_xWS_2 ($0 < x < 0.1$), which means that the r-WS_2 contains very little Li (<0.1 wt %).

The exfoliation-restacking process introduces considerable structural disorder in the MS_2 layers. X-ray diffraction and Raman spectroscopy studies have found that metal atoms in exfoliated (MS_2) monolayers have a distorted octahedral and not a perfect trigonal-prismatic coordination [3]. However, some confusion about the atomic ordering in bulk exfoliated-restacked metal dichalcogenides has arisen. Earlier studies have proposed that the *three-dimensional* structure is similar to that of trigonal TiS_2 type (i.e 1T-MoS_2).[11] Recent electron diffraction experiments, however, have suggested that the structure is similar to that of orthorhombic WTe_2.[12] These studies give the diffraction pattern of the (*hk*0) plane only and therefore yield a two-dimensional projection of the structure down the *c*-axis. However, no complete determination of the *three-dimensional* atomic structure, in terms of layer stacking, unit cell parameters, and atomic coordinates, has been accomplished with any of the studies carried out so far. This is an important scientific issue because a good knowledge of the structure is necessary to understand its guest−host properties, the electrochemical behavior, charge transport, and perhaps the catalytic properties of the MS_2 materials. This prompted us to undertake a study on the *three-dimensional* structure of bulk exfoliated-restacked metal dichalcogenides using novel experimental approaches.

Because single crystals of these materials cannot be obtained, and because powder diffraction techniques such as Rietveld refinement are of limited use (see below for reasons), we used the atomic pair distribution function (PDF) technique to solve the structure. The PDF technique has emerged recently as a powerful and unique tool for the characterization and structure refinement of crystalline materials with intrinsic disorder. The strength of the technique stems from the fact that it takes into account *the total diffraction*, that is Bragg as well as diffuse scattering, and so it can be applied to both crystalline[13] and amorphous materials.[14] In contrast, other techniques used to study polycrystalline samples (e.g. Rietveld)[15] use only the Bragg scattering portion of the pattern and therefore any information originating from the disorder present is lost. The limitations of the technique are that it is a powder technique, and like all powder diffraction the 3-D structure has to be inferred through modeling. Here we show that the structure of r-WS_2 is not a random turbostratic assembly of layers, as previously thought, but it can be better regarded as a monoclinic structure with considerable intrinsic disorder. This work presents independent and unequivocal confirmation that the structure of r-WS_2 is a disordered, low-symmetry variant of the structure WTe_2 and that W atoms in the layers associate into infinite parallel *zigzag* chains with W−W bond distances of 2.77(1) and 2.85(1) Å. This is an instructive example of the great potential of the PDF technique in determining the structure of crystalline materials with considerable intrinsic disorder.

2. Fundamentals of the PDF Technique

The atomic PDF, $G(r)$, is defined as follows:

$$G(r) = 4\pi r[\rho(r) - \rho_o] \tag{1}$$

where $\rho(r)$ and ρ_o are the local and average atomic number densities, respectively, and r is the radial distance. $G(r)$ is a measure of the probability of finding an atom at a distance r from a reference atom and so describes the atomic arrangement, i.e., structure, of materials. It is the Fourier transform of the experimentally observable total structure factor,[14] $S(Q)$, i.e.

$$G(r) = \left(\frac{2}{\pi}\right)\int_{Q=0}^{Q_{max}} Q[S(Q) - 1]\sin(Qr)\,dQ \tag{2}$$

where Q is the magnitude of the wave vector [$Q = 4\pi \sin(\theta)/\lambda$]. The structure factor is related to the coherent part of the total diffracted intensity of the material as follows:

$$S(Q) = 1 + \frac{[I^{coh}(Q) - \sum c_i|f_i(Q)|^2]}{|\sum c_i f_i(Q)^2|} \tag{3}$$

where $I^{coh}(Q)$ is the coherent scattering intensity per atom in electron units and c_i and f_i are the atomic concentration and X-ray scattering factor, respectively, for the atomic species of type *i*. The following important details of the PDF technique are to be noted: $G(r)$ is barely influenced by diffraction optics and experimental factors since these are accounted for in the step of extracting the coherent intensities from the raw diffraction data. This renders the PDF a *structure-dependent quantity* only. As *eq* 2 implies, *the total, not only Bragg diffracted*, intensities contribute to $G(r)$. In this way both the long-range atomic structure, manifested in the sharp Bragg peaks, and the local structural imperfections, manifested in the diffuse components of the diffraction pattern, are reflected in the PDF. Also, by accessing high values of Q, experimental $G(r)$ values with high real-space resolution can be obtained and, hence, quite fine

(7) (a) Heising, J.; Bonhomme, F.; Kanatzidis, M. G. *J. Solid State Chem.* **1998**, *139*, 22. (b) Brenner, J.; Marshall, C. L.; Ellis, L.; Tomczyk, N.; Heising, J.; Kanatzidis, M. G. *Chem. Mater.* **1998**, *10*, 1244. (c) Bissessur, R.; Schindler, J. L.; Kannewurf, C. R.; Kanatzidis, M. G. *Mol. Cryst. Liq. Cryst.* **1994**, *244*, A249. (d) Bissessur, R.; Heising, J.; Hirpo, W.; Kanatzidis, M. G. *Chem. Mater.* **1996**, *8*, 318. (e) Wang, L.; Schindler, J. L.; Thomas, J. A.; Kannewurf, C. R.; Kanatzidis, M. G. *Chem. Mater.* **1995**, *7*, 1753. (f) Bissessur, R.; Kanatzidis, M. G.; Schindler, J. L.; Kannewurf, C. R. *J. Chem. Soc., Chem. Commun.* **1993**, *20*, 1528. (g) Kanatzidis, M. G.; Bissessur, R.; DeGroot, D. C.; et al. *Chem. Mater.* **1993**, *5*, 595.

(8) Wyckoff, R. W. G. In *Crystal Structures*; John Wiley & Sons: New York, 1964.

(9) Schutte, W. J.; de Boer, J. L.; Jellinek, F. *J. Solid State Chem.* **1987**, *70*, 207.

(10) Heising, J.; Kanatzidis, M. G. *J. Am. Chem. Soc.* **1999**, *121*, 11720.

(11) Chianelli, R. R.; Scanlon, J. C.; Thompson, A. H. *Mater. Res. Bull.* **1975**, *10*, 1379.

(12) Heising, J.; Kanatzidis, M. G. *J. Am. Chem. Soc.* **1999**, *121*, 638.

(13) Petkov, V.; Jeong, I.-K.; Jung, J. S.; Thorpe, M. F.; Kycia, S.; Billinge, S. J. L. *Phys. Rev. Lett.* **1999**, *83*, 4089.

(14) Waseda, Y. In *The Structure of Noncrystalline Materials*; McGraw-Hill: New York, 1980.

(15) Rietveld, H. M. *J. Appl. Crystallogr.* **1969**, *2*, 65.

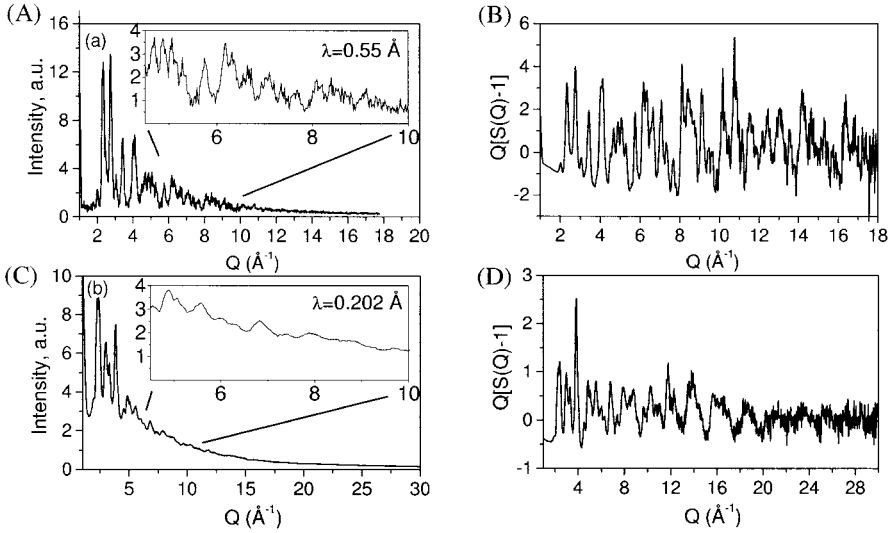

Figure 1. Powder diffraction patterns of hexagonal 2H-WS_2 and exfoliated-restacked WS_2 plotted as a function of Q: (A) raw diffraction intensity data for 2H-WS_2; (B) reduced $S(Q) - 1$ structure factor data for 2H-WS_2; (C) raw diffraction intensity data for r-WS_2; and (D) reduced $S(Q) - 1$ structure factor data for r-WS_2.

structural features revealed.[13] Therefore, the PDF can serve as a basis for structure determination. Once the PDF is obtained an approach similar to Rietveld refinement[15] is followed. A model atomic configuration is constructed and the respective PDF calculated and compared with the experimental one. Structural parameters in the model such as atomic positions, thermal factors, and occupancies are then varied in such a way as to improve the agreement between the calculated and experimental PDFs. This is done with, or without, observing predefined constraints imposed by the symmetry of the space group of the crystal structure being tested.[16] In this way, local distortions away from the average structure or lower, unresolved, symmetries can be modeled. The PDF is very sensitive to the coordination environment of atoms over short (<5 Å) and intermediate (5−20 Å) ranges. The approach has proven to be quite successful in determining the structure of various crystalline materials exhibiting different degrees of structural disorder.[17−19] For example, it was possible to measure the local Jahn−Teller distortion around Mn ions in $La_{1-x}Ca_xMnO_{3.0}$ for which Rietveld refinement showed only the average structure that is an ideal MnO_6 octahedron.[20] The PDF was employed here to study the *three-dimensional* structure of bulk exfoliated-restacked WS_2.

3. Experimental Section

3.1. Sample Preparation. Bulk r-WS_2 was obtained via the following three-stage process.[6,7,12] At first, a mixture of hexagonal WS_2 and $LiBH_4$ was reacted at 300−350 °C for 3 days. The reaction involves insertion of Li into WS_2 and oxidative decomposition of $LiBH_4$ as follows

$$WS_2 + x\mathrm{LiBH_4} \rightarrow \mathrm{Li}_x\mathrm{WS_2} + {}^1/_2 x\mathrm{B_2H_6} + {}^1/_2 x\mathrm{H_2} \qquad (4)$$

Then Li_xWS_2 was exfoliated in water and rinsed several times to remove the LiOH generated in the process. Finally, bulk product was obtained by centrifuging the suspension of monolayers and decanting the supernatant aqueous phase. The chemical composition of the material obtained and the relationship between charge on the single (WS_2) layers and structure of bulk r-WS_2 have been discussed extensively earlier.[10] The actual sample composition is Li_xWS_2 ($0 < x < 0.1$). Therefore, for the purposes of this study, r-WS_2 contains a negligible amount of Li.

3.2. X-ray Diffraction. Since no single crystals suitable for conventional diffraction experiments are obtained by the procedure described above, the sample was examined with powder X-ray diffraction. A complementary powder diffraction experiment on pristine, hexagonal WS_2 (2H-WS_2) was carried out for comparison. Both measurements were performed in symmetrical transmission geometry at room temperature. 2H-WS_2 was investigated with X-rays of energy 22 keV ($\lambda = 0.55$ Å). A laboratory setup equipped with an X-ray tube with Ag anode, a primary-beam *graphite* monochromator, and a Huber-type goniometer was employed for the experiment. The r-WS_2 was investigated with X-rays of energy 60 keV ($\lambda = 0.202$ Å) produced by the 24-pole wiggler at the A2 beam line of the Cornell High Energy Synchrotron Source (CHESS). The higher energy X-rays were used to extend the region of reciprocal space covered (i.e. to obtain data at very high Q values) and, hence, increase the resolution of PDF data in real space. The samples studied were uniform flat plates of loosely packed powder supported between Kapton foils. The thickness of the plates was optimized to achieve a sample absorption $\mu t \sim 1$, where μ is the linear absorption coefficient and t is the thickness of the sample for the respective radiation employed. The powders were back loaded and special care was taken to avoid the formation of texture. The diffraction data were collected by scanning at constant ΔQ steps of 0.02 Å^{-1} ($Q = 4\pi \sin(\theta)/\lambda$, and 2θ is the angle between the directions of the incoming and outgoing radiation beams). Several runs were conducted and the resulting patterns averaged to improve the statistical accuracy and reduce any systematic effects due to instabilities in the experimental setup. The raw diffraction patterns of 2H and r-WS_2 are shown in Figure 1A,C. The corresponding structure factor data $S(Q)$ derived from the raw data are shown in Figure 1B,D. Atomic PDFs were obtained from the raw diffraction data as follows. First, the raw diffraction data were corrected for background scattering, Compton scattering, and sample absorption. The corrected data were converted into absolute electron units and reduced to the structure factors $S(Q)$ as defined in eq 3. Finally, by applying the Fourier transformation of

(16) (a) Proffen, Th.; Billinge, S. J. L. *J. Appl. Crystallogr.* **1999**, *32*, 572. (b) The agreement fact is defined as $R\mathrm{wp} = \{\sum w_i(y_i^{\mathrm{obs}} - y_i^{\mathrm{calc}})^2/\sum(w_i y_i^{\mathrm{obs}})^2\}^{1/2}$.

(17) (a) Gutmann, M.; Billinge, S. J. L.; Brosha, E. L.; Kwei, G. H. *Phys. Rev. B* **2000**, *61*, 11762. (b) Proffen, Th.; DiFrancesco, R. G.; Billinge, S. J. L.; Brosha, E. L.; Kwei, G. H. *Phys. Rev. B* **1999**, *60*, 9973.

(18) Petkov, V.; DiFrancesko, R. G.; Billinge, S. J. L.; Acharaya, M.; Foley, H. C. *Phil. Mag.* **1999**, *B79*, 1519.

(19) (a) Toby, B. H.; Egami, T.; Jorgensen, J. D.; Subramanian, M. A. *Phys. Rev. Lett.* **1990**, *64* (20), 2414−2417. (b) Dmowksi, W.; Toby, B. H.; Egami, T.; Subramanian, M. A.; Gopalakrishnan, J.; Sleight, A. W. *Phys. Rev. Lett.* **1988**, *61* (22), 2608−2611.

(20) (a) Billinge, S. J. L.; DiFrancesco, R. G.; Kwei, G. H.; Neumeier, J. J.; Thompson, J. D. *Phys. Rev. Lett.* **1996**, *77*, 715. (b) Louca, D.; Egami, T. *Phys. Rev. B* **1999**, *59*, 6193.

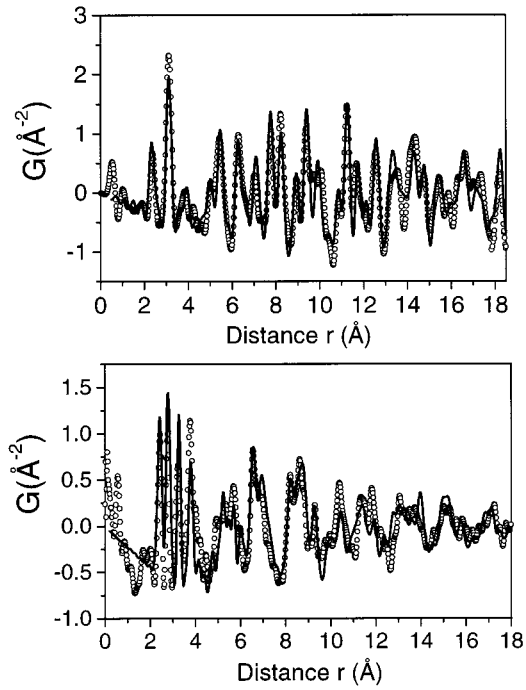

Figure 2. Atomic pair distribution functions, *G(r)*, of 2H-WS_2 (upper) and r-WS_2 (lower): experimental data, open circles; calculated data, solid line.

eq 2 the corresponding PDFs were computed. These are shown in Figure 2. All data corrections and data processing was carried out with the help of the program RAD.[21] A more detailed description of the essence of the PDF data processing procedures can be found in ref 14.

4. Results

Structure Determination. Even though the structure of 2H-WS_2 is well-known, it was used here as a standard to illustrate the capabilities of the PDF technique. As can be seen in Figure 1A,C the diffraction pattern of 2H-WS_2 consists of well-defined Bragg peaks—a characteristic of well-crystallized materials. The derived $S(Q)$ structure factor data, according to eq 3, are shown in Figure 1B,D. The corresponding PDF, shown in Figure 2, is also composed of well-defined peaks each pertaining to a given coordination sphere in the material. In particular, the first two peaks in the PDF, which are positioned at 2.41(1) and 3.18(1) Å, correspond to W−S atomic vectors within the WS_6 trigonal prisms and W−W vectors between neighboring prisms in 2H-WS_2, respectively. The third peak positioned at 3.61(1) Å corresponds to S···S pairs of atoms between the neighboring layers of (WS_6) trigonal prisms (see Figure 3). Thus the experimental PDF reflects well the main structural features of 2H-WS_2. A structural model based on the 8-atom hexagonal unit cell of 2H-WS_2 was fit to the experimental PDF and the structure parameters refined so as to obtain the best possible agreement between the calculated and experimental data. The fit was done with the help of the program PDFFIT[16] and it was constrained to have the symmetry of the $P6_3/mmc$ space group. The best fit achieved is shown in Figure 2 together with the corresponding weighted-pattern agreement factor R_{wp} defined in ref 16. The fit yielded the following structure parameters of 2H-WS_2: unit cell constants $a = 3.153(4)$ Å and $c = 12.343(5)$ Å, and atomic positions of W ($^1/_3$,$^2/_3$,$^1/_4$) and S ($^1/_3$,$^2/_3$,z) with $z = 0.625(5)$. The present structure parameters are in rather good agreement with those obtained by single-crystal diffraction experiments: $a = 3.1532(4)$ Å, $c = 12.323(5)$ Å, W ($^1/_3$,$^2/_3$,$^1/_4$), and S ($^1/_3$,$^2/_3$,z) with $z = 0.6225(6)$.[9] The excellent agreement well documents the fact that the atomic PDF is a reliable basis for structure determinations.

As can be seen in Figure 1 and as previous experiments have shown,[6,7] the diffraction pattern of r-WS_2 contains a few broad Bragg peaks and a pronounced diffuse component. This is made particularly evident by examining the inset in Figure 1A,C, which shows the intermediate range of the diffraction pattern on an expanded scale. Such a pattern, which is usually seen in materials with significant disorder, *is practically impossible to tackle by ordinary techniques for structure determination and refinement, such as the Rietveld technique*. The corresponding PDF, shown in Figure 2, is, however, rich in structure-related features and lends itself to real-space structure determination.

The PDF-based structure determination was carried out as follows. At first, the PDFs of 2H- and r-WS_2 were compared. The comparison strikingly demonstrates that hexagonal WS_2 and r-WS_2 do not share the same type of structure. The two materials have substantially different near atomic neighbor distributions, as demonstrated by the different number of peaks in the corresponding PDFs in the region of real space distances from 2 to 4 Å. The longer range atomic ordering in these materials also appears to be different as demonstrated by the different shape of the two PDFs at higher values of real-space distance r.

These experimental findings serve as independent evidence to rule out the trigonal-prismatic type atomic arrangement as a possible *three-dimensional* structure of restacked-exfoliated WS_2 since this model could not be reconciled with the measured PDF. Thus we attempted another trial structure. Recalling the findings of a previous electron diffraction experiment,[12] we considered the WTe_2 type structure. A structure model based on the 16-atom unit cell of WTe_2[22] was constructed and refined within the constraints of the space group $Pmn2_1$. This model was capable of reproducing the main features of the experimental PDF, however, though some discrepancies remained. The best fit to the experimental PDF that removed these discrepancies was obtained on the basis of a *monoclinic* unit cell being a distorted low-symmetry derivative of the unit cell of WTe_2. The results of this fit are presented in Figure 2. As can be seen in the figure the level of agreement between the PDF based on a monoclinic structure model and the experimental PDF (R_{wp} = 34%) of r-WS_2 is close to that achieved with the structure refinement of the standard compound 2H-WS_2 (R_{wp} =32%).[23] The fact that the distorted structure derived from that of WTe_2 gives a comparable R_{wp} value to the one obtained from the refinement of 2H-WS_2 supports the notion that the monoclinic structure is a good representation of the three-dimensional atomic ordering in exfoliated-restacked WS_2. This is a significant

(21) Petkov, V. *J. Appl. Crystallogr*. **1989**, *22*, 387.

(22) Mar, A.; Jobic, S.; Ibers, J. A. *J. Am. Chem. Soc*. **1992**, *114*, 8963.

(23) (a) The agreement factors, R_{wp}, reported here appear high when compared to agreement factors reported with single crystal and Rietveld refinements. This does not indicate an inferior structure refinement but merely reflects the fact that the PDF function being fit is not the same one typically fit in a Rietvelt refinement and is a much more sensitive quantity. For reference, the best PDFs fits ever achieved usually yield R_{wp} = 15 to 20% (see refs 18 and 23b) and a fit with R_{wp} = 30% is still considered quite successful. In PDF analysis one typically works with the atomic distribution function $G(r) = 4\pi r[\rho(r) - \rho_o]$, which is the Fourier transform of the so-called reduced structure factor $Q[S(Q) - 1]$, where $\rho(r)$ and ρ_o are the local and average atomic number density and Q is the wave vector. The extra Q/r "pre-factors" turn the $Q[S(Q) - 1]/G(r)$ couple a very sensitive quantity. Note, Rietveld refinement relies on something analogous to $S(Q)$. A formula analogous to the one used in Rietveld is $R_p = \{\Sigma|y_i^{obs} - y_i^{calc}|/\Sigma(y_i^{obs})\}$. Agreement factors based on this formula are 10% for 2H-WS_2 and 12% for r-WS_2. (b) Gutmann, M.; Billinge, S. J. L.; Brosha, E. L.; Kwei, G. H. *Phys. Rev. B* **2000** in press; http://xxx.lanl.gov/abs/cond-mat/9908365.

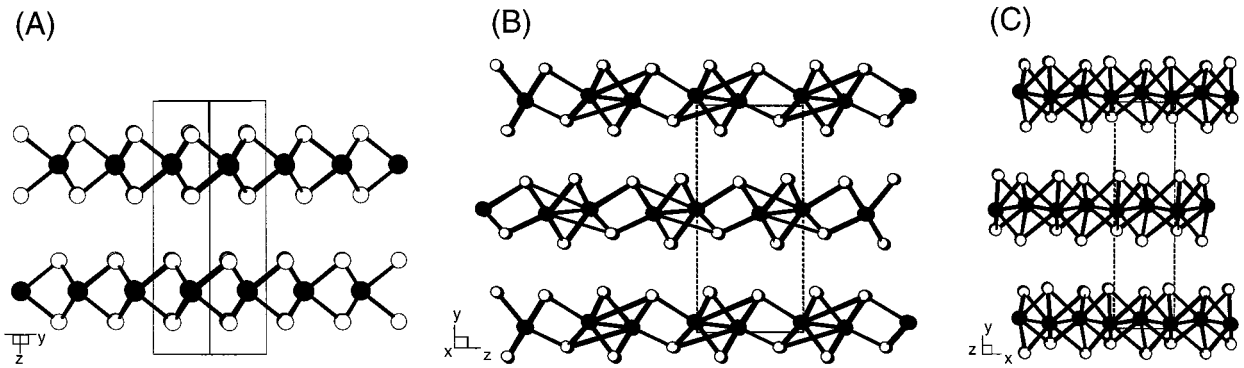

Figure 3. (A) View down the *a* axis of hexagonal, (B) r-(monoclinic)WS_2 viewed down the *b*-axis along the direction of the *zigzag* chains, and (C) r-WS_2 viewed down the *c*-axis. The large black circles are W atoms and the small open ones are S atoms.

Table 1. Positional parameters (*x*,*y*,*z*) and isotropic thermal factors U_{iso} of W and S in monoclinic WS_2[a]

	x	*y*	*z*	U_{iso} (Å^2)
W(1)	0.052(2)	0.604(2)	0.518(2)	0.0053(3)
W(2)	0.446(3)	−0.002(2)	0.040(2)	0.0053(3)
S(1)	0.082(4)	0.870(4)	0.672(4)	0.0061(3)
S(2)	0.546(4)	0.641(4)	0.160(4)	0.0061(3)
S(3)	0.542(4)	0.234(4)	−0.113(4)	0.0061(3)
S(4)	0.047(4)	0.215(4)	0.431(4)	0.0061(3)

[a] Please note that both W and S occupy the Wyckoff position (*2a*) in *S.G.* $P112_1$.

result demonstrating that the PDF technique can be confidently applied in structure determination studies.

According to the present PDF study the *three-dimensional* structure of r-WS_2 is well described in the monoclinic system (*S.G.* $P112_1$) with four formula units in a cell with parameters $a = 3.270(5)$ Å, $b = 5.717(5)$ Å, $c = 12.309(5)$ Å, and $\gamma = 88.48°$.[24] The refined positions of W and S atoms are listed in Table 1. Fragments of atomic-scale structures of 2H-WS_2 and r-WS_2 are shown in Figure 3.

5. Discussion

An important outcome of the present structural study is that the diffraction data of r-WS_2 can be fit well with a relatively simple, three-dimensional structure model. This unambiguously shows that r-WS_2 still possesses a significant degree of *three-dimensional* order, i.e., it is not simply a turbostratic pile-up of (WS_2) monolayers, something which was not fully appreciated initially.[3−7] A pile-up of turbostratically disordered layers would give rise to a PDF yielding only the two-dimensional structure with no out-of-plane atomic correlations present, as observed in pyrolytic graphite.[18]

An analysis of the refined structure parameters of Table 1 and an inspection of Figure 3 show that r-WS_2 is a layered material just like 2H-WS_2. The individual layers are stacked along the *c*-axis of the monoclinic unit cell and the closed approach between adjacent layers is through sulfur atoms S2 and S3 at 2.9 Å. The corresponding distance in 2H-WS_2 is longer at 3.61 Å because of the A...A stacking arrangement of the S atoms. Interestingly, the distance between W atoms from neighboring layers does not seem to change accordingly: it is

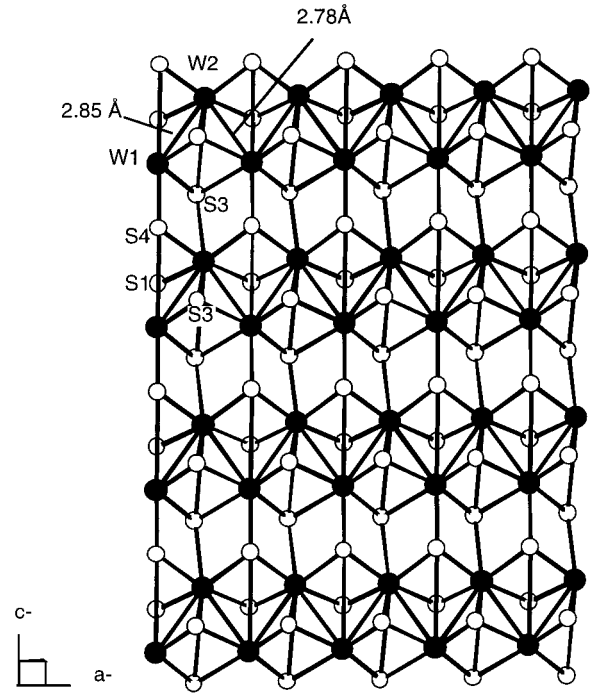

Figure 4. View of a layer of r-WS_2. The large black circles are W atoms and the small open ones S atoms. *Zigzag* chains (thin lines) of W atoms run in parallel to the *a*-axis of the monoclinic unit cell.

6.28 and 6.51 Å in the exfoliated-restacked and 2H-WS_2, respectively.

Another substantial difference between the structures of exfoliated-restacked WS_2 and 2H-WS_2 comes from the different spatial arrangement of the W atoms. In 2H-WS_2 the metal atoms occupy the vertices of regular hexagonal sublattices and are all separated by the same distance of 3.18 Å. Metal atoms in r-WS_2 occupy two distinct positions in the monoclinic unit cell, giving rise to well-defined infinite zigzag chains of W atoms. As a result, four distinct W−W atomic pair distances occur: 2.77 and 2.85 Å along the chain direction, 3.85 Å along *b*, and 3.27 Å along the *a*-axis of the monoclinic unit cell, respectively (see Figure 3). These distinct W−W atomic pairs are the main contributors to the first four well-defined peaks in the experimental PDF (see Figure 2). Also, when considered within a single layer, these distinct W−W pairs form parallel zigzag chains along the *a*-axis of the unit cell via metal−metal bonds of length 2.77 and 2.85 Å (see Figure 4). The observation of two different W−W distances within the zigzag chains is surprising and was not detected by the earlier electron diffraction study.[12]

(24) A key point here is that the space group we propose for the structure is a working model since it is really very difficult to extract symmetry information from the PDF technique. This is straightforward when done with Bragg peaks. We can say with certainty, however, that a lower symmetry is needed than that of the pristine material, and the one that gives a satisfactory model is $P2_1$. From a practical point of view, it is easier solving a structure using PDF analysis if a fairly good trial structure exists, in this case WTe_2.

Exfoliated-restacked WS_2 and 2H-WS_2, however, also differ greatly in the type of W−S coordination polyhedra that build the respective single layers. While in 2H-WS_2 the layers are built of fairly perfect (WS_6) trigonal prisms[9] and there is only one type of first neighbor W−S distance of 2.40 Å, those in r-WS_2 are built of quite distorted (WS_6) octahedra, where the first neighbor W−S distances vary from 2.30 to 2.70 Å. The change in the type of the W−S coordination polyhedron is also well demonstrated by the values of S−W−S bond angles. While there is a unique S−W−S bond angle of 82.5° in trigonal-prismatic WS_2, bond angles ranging from 77° to 114° occur in exfoliated-restacked WS_2. The distortion in the W−S_6 polyhedron reflects the departure of the *W* atoms from the positions in the original hexagonal lattice and their shift toward each other to form metal−metal bonds and zigzag chains. The change in the (WS_6) coordination polyhedra and the concurrent formation of W−W chains is what accounts for the different type of electrical conductivity exhibited by the two materials.[5,7,12]

As the theoretical calculations of Mattheis show[25] and as already discussed by Zhou et al.[26] the density of d-states is different for trigonal-prismatic (2H-WS_2) and octahedral coordination (1T-WS_2) of metal atoms. A subband that contains only two states exists when metal atoms are with trigonal-prismatic coordination. This subband is filled and an energy band gap of about 1.8 eV separates it from the upper unoccupied band in 2H-WS_2 giving rise to a semiconductor. In the octahedral phase the lower subband contains six states per metal atom. Since only two of them are occupied, r-WS_2 should exhibit metallic behavior as observed.[5,7] Since, however, the latter is severely distorted from 1T-WS_2, electronic band calculations should be performed on this system as well.

5. Conclusion

The atomic PDF analysis is a useful technique to determine the *three-dimensional* structure of crystalline materials with considerable intrinsic disorder. The strength of the PDF technique derives from the fact that it takes into account the entire scattering pattern, i.e., both Bragg and diffuse. The exfoliation-restacking process introduces serious local disorder in bulk WS_2, which raises an important scientific issue as to the structure of this material. We believe that the present PDF study lays this issue to rest by elucidating the three-dimensional structure. This is best modeled by reducing the average symmetry of the unit cell from hexagonal to monoclinic. The material, however, retains its layered-type atomic ordering. Previous notions that the layers are turbostratically disordered in r-WS_2 are not supported by the experimental data. In a truly turbostratic stacking arrangement the layers are randomly oriented as they pile up. Instead, the structure of exfoliated-restacked WS_2 is more ordered than that. Not only the coordination of metal atoms changes from trigonal-prismatic to distorted octahedral, but also, within the layers, the W atoms form short W−W bonds and infinite parallel *zigzag* chains, which is a radical departure from the hexagonal organization in the pristine material. This explains why semiconducting 2H-WS_2 turns into a p-type metal upon exfoliation and restacking.[12]

By extension, similar conclusions are expected for restacked MoS_2 layers; however, the more kinetically labile nature of this material[27] (i.e. it partially converts to 2H-MoS_2 in the period of days) prevented us from studying it in detail. This would be the subject of a future PDF study designed to deal with the kinetic problem.

Acknowledgment. Thanks are due to Dr. S. Kycia for the help with the experiments. The work was supported by NSF grant CHE 99-03706 (Chemistry Research Group) and DMR-9817287. CHESS is operated by NSF through grant DMR-9713242.

JA002048I

(25) Mattheiss, L. F. *Phys. Rev.* **1973**, *B8*, 3719.

(26) Zhou, X.; Yang, D.; Frindt, R. F. *J. Phys. Chem. Solids* **1996**, *57*, 1137.

(27) Bissessur, R. Ph.D. Thesis, Michigan State University, 1994.